

Research Paper

Bioactive Scaffolds for Regeneration of Cartilage and Subchondral Bone Interface

Cuijun Deng^{1,2}, Huiying Zhu¹, Jiayi Li³, Chun Feng^{1,2}, Qingqiang Yao³, Liming Wang³, Jiang Chang¹, Chengtie Wu¹✉

1. State Key Laboratory of High Performance Ceramics and Superfine Microstructure, Shanghai Institute of Ceramics, Chinese Academy of Sciences, Shanghai 200050, P.R.China
2. University of Chinese Academy of Sciences, Beijing 100049, P.R.China
3. Department of Orthopaedic Surgery, Digital Medicine Institute, Nanjing Medical University Nanjing Hospital. No. 68 Changle Road, Nanjing 210006, P.R.China

✉ Corresponding author: Email: chengtiewu@mail.sic.ac.cn (C. Wu); Tel: +86-21-52412249; Fax: +86-21-52413903

© Ivyspring International Publisher. This is an open access article distributed under the terms of the Creative Commons Attribution (CC BY-NC) license (<https://creativecommons.org/licenses/by-nc/4.0/>). See <http://ivyspring.com/terms> for full terms and conditions.

Received: 2017.11.25; Accepted: 2018.01.17; Published: 2018.02.15

Abstract

The cartilage lesion resulting from osteoarthritis (OA) always extends into subchondral bone. It is of great importance for simultaneous regeneration of two tissues of cartilage and subchondral bone. 3D-printed $\text{Sr}_5(\text{PO}_4)_2\text{SiO}_4$ (SPS) bioactive ceramic scaffolds may achieve the aim of regenerating both of cartilage and subchondral bone. We hypothesized that strontium (Sr) and silicon (Si) ions released from SPS scaffolds play a crucial role in osteochondral defect reconstruction.

Methods: SPS bioactive ceramic scaffolds were fabricated by a 3D-printing method. The SEM and ICPAES were used to investigate the physicochemical properties of SPS scaffolds. The proliferation and maturation of rabbit chondrocytes stimulated by SPS bioactive ceramics were measured *in vitro*. The stimulatory effect of SPS scaffolds for cartilage and subchondral bone regeneration was investigated *in vivo*.

Results: SPS scaffolds significantly stimulated chondrocyte proliferation, and SPS extracts distinctly enhanced the maturation of chondrocytes and preserved chondrocytes from OA. SPS scaffolds markedly promoted the regeneration of osteochondral defects. The complex interface microstructure between cartilage and subchondral bone was obviously reconstructed. The underlying mechanism may be related to Sr and Si ions stimulating cartilage regeneration by activating HIF pathway and promoting subchondral bone reconstruction through activating Wnt pathway, as well as preserving chondrocytes from OA via inducing autophagy and inhibiting hedgehog pathway.

Conclusion: Our findings suggest that SPS scaffolds can help osteochondral defect reconstruction and well reconstruct the complex interface between cartilage and subchondral bone, which represents a promising strategy for osteochondral defect regeneration.

Key words: 3D-printing, strontium, osteoarthritis, osteochondral defects, cartilage regeneration.

Introduction

As a translucent elastic tissue, articular cartilage adheres to subchondral bone [1, 2]. OA is the most common disease that causes articular cartilage degradation and lesion [3]. Numerous surgical therapeutic methods, such as micro-fracturing and mesenchymal stem cell implantation methods [4-6],

have been raised to regenerate cartilage over the years. Nevertheless, the drawbacks, for example the secondary trauma and low survival rate of exogenous stem cells, restricted the effective regeneration capability of these approaches. As cartilage has no vasculature and lymphatic, and mature chondrocytes

possess limited proliferation and migration ability, thus cartilage regeneration remains a significant challenge. Moreover, the cartilage lesion always involves in the subchondral bone and develops into osteochondral defect [7]. The reality suggests that simultaneously reconstructing cartilage and subchondral bone is of great importance for OA osteochondral defect regeneration. Since cartilage and subchondral bone possess different physiological functions, it remains a major problem to develop one single scaffold that can biologically meet the need for simultaneously reconstructing both of cartilage and subchondral bone within osteochondral defects.

It has been proved that the subchondral bone tissue plays a significant role in OA onset and progression [8]. Our previous studies showed that bioactive ceramics could promote both of the subchondral bone and cartilage regeneration [9, 10]. Numerous implantation materials, including monophasic, biphasic and triphasic scaffolds, have been manufactured for regeneration of osteochondral defects [11-14]. However, poor mechanical properties and insufficient biological activities have hampered their further application for the scaffolds. To mimic the natural structures and properties of cartilage and subchondral bone, various multilayered structures, such as biphasic and triphasic, have been fabricated. Nevertheless, due to the complex interface microstructure between cartilage and subchondral bone, it is almost impossible to biologically mimic the original structure and physiological functions of osteochondral tissue [15-17]. Moreover, the adjacent two layers might be delaminated due to insufficient bonding force between them. Hence, developing an intelligent scaffold with bi-lineage biological properties to fulfill the requirements for the complex interface microstructure between cartilage and subchondral bone reconstruction is quite urgent.

It is known that Sr is an essential trace element, which plays an important role for maintaining human tissue functions, especially for bone. Previous studies showed Sr could enhance the osteoconductive property of calcium phosphates and elevate the mechanical property of bone tissue [18]. Moreover, Sr has been reported to promote osteoblast differentiation, as well as inhibit osteoclast formation and resorption [19, 20]. In addition, Sr plays a crucial role in reducing cartilage degeneration and decreasing chondrocyte apoptosis on the osteoarthritis therapy [21, 22]. Recent study proved that Sr significantly promoted the early chondrogenic differentiation of dedifferentiated fat cells [23].

Si is an important nutrient element in human body, which plays a key role in healthy connective tissue, such as articular cartilage and bone [24]. It was

reported that Si, involved in the mineralization process of new bone formation, could promote skeletal growth and development [25]. Furthermore, Si could stimulate cartilage extracellular matrix synthesis and integrity [26-28], as well as promote the proliferation and osteogenic differentiation of rabbit mesenchymal stem cells (rBMSCs) [29, 30]. In addition, Si was reported to have positive effect on osteoarthritis therapy [31].

As previously stated, both Sr and Si have beneficial impacts on chondrocytes and rBMSCs. In order to combine the beneficial effect of Sr and Si ions, a Sr and Si containing bioactive ceramic was fabricated. We supposed that the bioactive scaffolds containing Sr and Si ions are beneficial for osteochondral defect reconstruction and restore the interface microstructure between cartilage and subchondral bone, as well as protect cartilage from degeneration in OA. SPS scaffolds were used to investigate their osteochondral regeneration *in vitro* and *in vivo*, and the underlying mechanism for Sr and Si ions protecting cartilage from OA and stimulating osteochondral reconstruction was further investigated.

Materials and Methods

Materials

Strontium oxide (SrO) and silicon dioxide (SiO₂) were bought from Aladdin (China) and Sinopharm Group Co. Ltd (China), respectively. Ammonium dihydrogenphosphate (NH₄H₂PO₄) and sodium alginate were provided by Alfa Aesar (USA). Pluronic F-127 (20 wt %) was obtained from Sigma-Aldrich(USA),and tricalcium phosphate (TCP) ceramics were purchased from Kunshan Chinese Technology New Materials Co., Ltd.

Fabrication and characterization of SPS scaffolds

Pure Sr₅(PO₄)₂SiO₄ (SPS) bio-ceramics were synthesized by a solid-state reaction method, and SPS scaffolds were manufactured by using a 3D plotting device (Dresden, Germany) with a computer assist design (CAD) model. We mixed the sodium alginate and SPS powders in a mass ratio of 3:100, then added 20 wt% F-127 (Ploxamer) in the mixture and stirred until becoming homogeneous. Subsequently, the paste was loaded into the printing tube and extruded through nozzles (needle standard: 22 G) to fabricate a primary scaffold. To obtain SPS scaffolds, the primary scaffolds were dried over night at room temperature and then sintered at 1450°C for 3 h. Also, we prepared TCP scaffolds in the same way, which was used as a control group. Macro-photograph and surface

morphology of SPS scaffolds were obtained from optical microscopy (S6D, Leica, Germany) and scanning electron microscope (SEM, SU8220, HITACHI, Japan), respectively. Micro-CT images and porosity of the scaffolds were obtained from a SKYSCAN 1173 CT scanner (Bruker, Germany). To assay the Sr, Si, Ca ions release from SPS scaffolds, the scaffolds were soaked in Dulbecco's modified Eagle's medium low-glucose (DMEM) (Thermo Fisher Scientific, Grand Island, America) for 1, 2, 7, 11, 14, 21, 28, 35 and 42 days in a 37°C shaking water bath. A ratio of 200 mg/mL was used to add scaffold mass to DMEM volume. At the setting different time points, a pH meters (PHSJ-4A, Leici Co., Ltd., Shanghai, China) was used to measure the average pH value, and inductively coupled plasma atomic emission spectroscopy (ICPAES; Varian, USA) was used for Sr, Si and, Ca ions assessment.

Cell culture experiments with chondrocytes

Chondrocytes from one month old rabbit knee growth plate were obtained from Nanjing Medical University Nanjing Hospital, and the use of the cells for the *in vitro* study got permission from the ethics commission of Nanjing Medical University. The DMEM contained 10% fetal calf serum (Thermo Fisher Scientific), 100 µg/mL streptomycin and 100 U/mL penicillin (Thermo Fisher Scientific) was used for chondrocytes culturing. The cells were cultured in an incubator with 5% CO₂ at 37°C.

The stimulatory effect of SPS extracts on the proliferation and maturation of chondrocytes

Extracts of SPS and TCP were prepared according to the following steps: the ratio of SPS or TCP mass to DMEM volume was 200 mg/mL and the mixture was vibrated at 37°C for 24 h with a speed of 120 rpm. Subsequently, the mixture was centrifuged at a speed of 4000 rpm and filtrated with 0.22 µm filters. Lastly, the original extracts (200 mg/mL, set as 1) of SPS and TCP were diluted into 1/2 (100 mg/mL), 1/4 (50 mg/mL), 1/8 (25 mg/mL), 1/16 (12.5 mg/mL), 1/32 (6.25 mg/mL) and 1/64 (3.125 mg/mL), respectively. To analyze the concentrations of Sr, Si and, Ca ions, ICP-AES analysis was used. A CCK-8 (cell counting kit-8, Beyotime, China) assay was used to analyze the proliferation of chondrocytes. Extracts of SPS bio-ceramics were prepared and chondrocytes were inoculated for 1, 3, 7 days in 96-well plates. Subsequently, chondrocytes were incubated with 10% CCK-8 reagent diluted by DMEM for 2 h in 5% CO₂ incubator at 37°C. The OD values were obtained from a multifunction microplate reader (Spectra Fluor Plus, Tecan, Crailsheim, Germany) at 450 nm.

To analyze the mRNA transcript level of chondrocytes specific genes (COL II, Aggrecan, SOX9 and N-cadh), the total RNA was collected by using an RNA prepare Micro Kit (TaKaRa, Japan). After measured at 260 nm with a multifunction microplate reader (Spectra Fluor Plus, Tecan, Crailsheim, Germany), the total RNA was reverse into cDNA by using a Prime Script 1st Strand cDNA synthesis kit (TOYOBO, Japan). Subsequently, RT-qPCR (Quantitative real-time reverse transcriptase polymerase chain reaction) analysis was conducted by using a SYBR Green QPCR Kit (TaKaRa, Japan) with a Light Cycler apparatus (Bio-rad, CFX-Touch) as the following protocol: firstly, reverse transcription at 60°C for 20 min; secondly, activation of Hot Star Taq DNA polymerase/inactivation of reverse transcriptase at 95°C for 1 min; the last, 40 cycles of 95°C for 15 s, 60°C for 15 s, and 72°C for 45 s. To calculate the relative expression levels of target genes a 2^{-ΔΔCt} method was conducted. The relative gene expression levels of blank control were set as 1, and GAPDH gene was selected as a reference gene. Oligo 7.0 software was used to design primer sequences (BioSune Biotechnology Co., Ltd, Shanghai, China) and the primer sequences were summarized in Table S1.

SPS extracts promoted the expression of type II collagen protein in chondrocytes

The SPS extracts were used to culture chondrocytes for 3 days in an incubator with 5% CO₂ at 37°C. According to the manufacturer's protocol, a type II collagen staining kit (Abcam, USA) was applied to measure the expression of type II collagen protein in chondrocytes. In brief, chondrocytes were anchored with 2.5% glutaraldehyde (Sinopharm Group Co. Ltd., China), following by incubated with 1% bovine testicular hyaluronidase. Subsequently, chondrocytes were treated with primary antibody (5 µg/mL, Abcam, ab3092) and second antibody (1 µg/mL, Abcam, ab175472) according to the manufacturer's protocol. Lastly, cytoskeleton and nuclei were stained with FITC (fluorescein isothiocyanatephalloidin, Sigma-Aldrich, USA) and DAPI (4',6-diamidino-2-phenylindole, Sigma-Aldrich, USA), respectively. Images were obtained with an Argon laser line of 405 nm (DAPI channel, blue), 488 nm (FITC channel, green) and 568 nm (COL II channel, yellow). The collected and analysed number of CLSM images was 3. An image pro-plus 6 software was used for quantification of COL II protein.

The western blot analysis was further conducted to evaluate the expression of COL II protein. In brief, after the chondrocytes were cultured with SPS extracts for 3 days, the whole-cell extracts were prepared by using a protein extract kit (P0027,

Beyotime, China). The total protein from each sample was separated on SDS-PAGE gels, and then transferred onto a nitrocellulose membrane. After being blocked for 1 h, the nitrocellulose membranes were incubated with the primary antibodies against COL II and GAPDH (antibodies against COL II and GAPDH were Santa Cruz Biotechnology) overnight, and then incubated with the corresponding fluorescent secondary for 1 h (LI-COR Biosciences, USA). Finally, Odyssey CLx was used to observe the protein bands (LI-COR Biosciences, USA).

Stimulated effect of Sr and/or Si ions on the maturation of chondrocytes *in vitro*

The method we used to prepare different concentrations of Sr and/or Si ions solution was the same with that we prepared SPS extracts. SrO and mesoporous silica were used to obtain Sr and Si ions, respectively. SrO was bought from Aladdin (China) and mesoporous silica was self-made. An ICP-AES method was used to analyze the concentrations of Sr and Si ions. After chondrocytes were cultured with Sr and/or Si ions solutions for 3 days, the total RNA was extracted. And the expression of related genes (COL II, Aggrecan, SOX9 and N-cadh) of chondrocytes and genes in HIF-1 α pathway was measured. In order to investigate the stimulatory effect of Sr and/or Si ions on type II collagen protein expression, confocal laser scanning microscope (CLSM) was used. After culturing with Sr and/or Si ions solutions, chondrocytes were treated by using the method we described before. CLSM images were acquired from an Argon laser line of 405 nm (DAPI channel, blue), 488 nm (FITC channel, green) and 568 nm (COL II channel, yellow). The collected and analysed number of CLSM images was 3. An image pro-plus 6 software was used for quantification of COL II protein. Furthermore, the western blot analysis was performed to investigate the COL II protein of chondrocytes cultured with Sr and/or Si ions solutions.

The underlying mechanism of Sr and/or Si ions preserved chondrocytes from OA *in vitro*

The related genes of matabolic activity (MMP3, MMP13 and Adamts-5) and autophagy markers (P62, Atg5, Atg12 and Atg16L1), as well as Indian hedgehog pathway (IHH, Patched-1 and Gli-1) were investigated in order to explore the underlying mechanism of Sr and/or Si ions protected chondrocytes from OA. Before Sr and/or Si ions were added to culture with chondrocytes, interleukin-1 β (IL-1 β , 10 ng/mL) was used to fabricate an OA model of chondrocytes. In OA chondrocytes the smoothed antagonist (SANT-1, 5 μ M) was used to inhibit IHH

signaling and fabricated a positive control group. After culturing for 3 days, the total RNA was extracted and related genes were investigated. Oligo 7.0 software was used to design primer sequences (BioSune Biotechnology Co., Ltd, Shanghai, China) and the primer sequences were summarized in Table S1.

The adhesion and proliferation of chondrocytes in SPS scaffolds

To evaluate the proliferation of chondrocytes in SPS scaffolds, a CCK-8 kit was used. After the chondrocytes were seeded in SPS scaffolds for 1, 3 and 7 days, 10% CCK-8 solution was used to incubate the cells for 2 h. The absorbance of the CCK-8 solution was measured with a multifunction microplate reader at 450 nm. In order to observe the morphology of chondrocytes in SPS scaffolds, SEM and CLSM were used. After chondrocytes were seeded in SPS scaffolds and incubated for 1 day, the cells were fixed with 2.5% glutaraldehyde and dehydrated in graded ethanol (30, 40, 50, 60, 70, 80, 90, 95, 100, 100, 100 v/v %) as well as treated with hexamethyldisilazane (HDMS) (Sinopharm Chemical Reagent Co., Ltd, China). A SU8220 SEM (HITACHI, Japan) was used to obtain the morphological characteristics of cells. Before cells were observed with CLSM, 4',6-diamidino-2-phenylindole (DAPI, Sigma-Aldrich, USA) and fluorescein isothiocyanatephalloidin (FITC, Sigma-Aldrich, USA) were used to stain the nuclei and cytoskeleton, respectively. Lastly, we used an Argon laser line of 405 nm (DAPI channel, blue) and 488 nm (FITC channel, green) to obtain CLSM images.

***In vivo* regeneration of cartilage and bone for SPS scaffolds**

All New Zealand rabbits were handled according to the guidelines authorized by the Nanjing Medical University Ethics Committee. An osteochondral defect model was created in eighteen eligible rabbits (2-2.5 kg, 3 months old) for evaluating the regeneration effect of SPS and TCP scaffolds. After general anesthesia, osteochondral defects (diameter: 4 mm, height: 5 mm) were created on the groove of knees, and then the SPS or TCP scaffold (n=6 for each group) was implanted into the defect, the blank control group was untreated. After surgery, all of the rabbits were treated with Penicillin for five days and stayed singly in cages. The knee joints were collected for gross observation and Micro-CT analysis, as well as histological analysis after the rabbits were sacrificed at 8 and 12 weeks post-surgery. Subsequently, regeneration tissues were assessed with the international cartilage repair society (ICRS) macroscopic assessment scale by three observers.

Furthermore, a Micro-CT scanner (Bruker, Germany) was used to obtain the relative bone volume fraction (BV/TV) and trabecular thickness (Tr. Th) as well as reconstruction images. In addition, Hematoxylin-eosin (HE), Safranin-O/Fast Green (Safranin-O) and Toluidine blue (TB) were used to stain six PMMA specimens from each group to further investigate the regeneration effect, respectively.

Statistical Analysis

All of the experimental data were presented as means \pm standard deviation (SD) and conducted by one-way ANOVA with a post hoc test. A value of $p < 0.05$ was considered statistically significant and the data were indicated with (*) for $0.01 < p < 0.05$, (**) for $0.001 < p < 0.01$, and (***) for $p < 0.001$.

Results

Analysis of Sr, Si and Ca ionic concentrations in SPS extracts

The ionic concentrations of Sr, Si, Ca and P in SPS extracts are shown in Table 1. The concentration of Sr and Si ions was 0.04 and 0.06 mg/L in CTR, respectively. While the concentration of Sr and Si ions in SPS extracts was gradually elevated as the extract concentrations increased from 3.125 to 200 mg/mL. The Ca and P in SPS extracts were mainly within the range 13-73 mg/L and 11-32 mg/L, respectively.

Characterization of SPS scaffolds

Digital photographs and SEM images of TCP and SPS scaffolds were shown in Figure 1. The controllable structure and uniform macropores of TCP and SPS scaffolds were prepared via a 3D-printing method (Figure 1A, B and, Figure S1). The SEM images further verified that the 3D-printing scaffolds had uniform macropore morphology (Figure 1C, D), the high magnification images exhibited the size of crystalline grains of SPS scaffolds were above 5 μm , which were much greater than that of TCP scaffolds (Figure 1E, F).

The original pH value of DMEM is ~ 8.2 , while the pH value of DMEM was ~ 8.5 and ~ 8.7 after soaking TCP and SPS scaffolds for 1 day, respectively. The pH values decreased gradually with soaking time prolonging, and the pH value of DMEM was ~ 8.2 after soaking TCP and SPS scaffolds for 42 days, which was closed to the original pH value of DMEM (Figure 2A). It can be found in Figure 2 that SPS scaffolds maintained a sustained release of Si and Sr ions. The Ca ions released from TCP scaffolds was ~ 0.8 mg, while there were no Ca ions released from SPS scaffolds after soaking for 42 days (Figure 2B). Furthermore, the Si and Sr ions released from SPS scaffolds was ~ 0.1 mg and ~ 0.3 mg respectively, while

there were no Si and Sr ions released from TCP scaffolds after soaking for 42 days (Figure 2C, D).

Stimulatory effects of SPS extracts on chondrocytes *in vitro*

The results of CCK-8 assay exhibited that the proliferation of chondrocytes cultured with SPS and TCP extracts has no significant difference with the CTR (blank control) groups (Figure S2). RT-qPCR analysis displayed that SPS extracts distinctly elevated the chondrocytes specified genes (COL II, Aggrecan, SOX9 and N-cadh) expression within the concentration range of 3.125-50 mg/mL at day 3 and 7 as compared to that of CTR and TCP groups (Figure 3). Furthermore, the expression of COL II protein in chondrocytes was also enhanced (Figure 4). Results of western blot demonstrated that the COL II protein expression in chondrocytes of SPS groups was significantly higher than that of CTR and TCP groups at the concentration of 50 mg/mL.

The stimulatory effect of Sr and/or Si ions on the maturation of chondrocytes

Base on the study of Sr and Si ions concentration in SPS extracts, the chondrocytes response to the culture medium which contained different concentrations of Sr and Si ions was further investigated (Figure 5). Sr ions enhanced chondrocyte typical markers expression by activating HIF-1 α pathway within the concentration range of 0.25-4 mg/L. Furthermore, Sr and Si ions distinctly elevated COL II, Aggrecan, SOX9, N-cadh expression within the concentration range of Sr ions 0.25-4 mg/L and Si ions 0.5-8 mg/L, respectively. In addition, the expression of COL II gene was significantly increased by Sr and Si ions at the concentration of Sr ions 0.25 mg/L and Si ions 0.5 mg/L. The expression level of Aggrecan gene was elevated by Sr and Si ions together within the concentration range of Sr ions 1-4 mg/L and Si ions 2-8 mg/L, as well as the expression of SOX9 gene was enhanced by Sr and Si ions at the concentration of Sr ions 4 mg/L and Si ions 8 mg/L. Also, N-cadh gene was stimulated by Sr and Si ions cooperatively within the concentration range of Sr ions 0.25-2 mg/L and Si ions 0.5-4 mg/L.

Moreover, to evaluate the stimulatory effect of Sr and Si ions on chondrocytes, the expression of COL II protein was further evaluated (Figure 6). The results showed that Sr ions enhanced the expression of COL II protein in chondrocytes within the concentration range of 0.25-4 mg/L, and that of Si ions 0.5-8 mg/L. Interestingly, Sr and Si ions together promoted COL II protein expression within the concentration range of Sr ions 0.25-1 mg/L and Si ions 0.5-2 mg/L.

Table 1. The ionic concentrations of Sr, Si, Ca and P in SPS extracts

Ionic Con. (mg/L)	Powders extracts concentrations (mg/mL)							
	0 (CTR)	3.125	6.25	12.5	25	50	100	200
Sr	0.04±0.01	0.79±0.10	1.54±0.10	2.86±0.21	5.39±0.30	10.47±1.15	19.19±2.06	35.96±3.85
Si	0.06±0.01	1.80±0.01	3.54±0.01	6.99±0.14	13.97±0.47	27.28±1.17	54.38±2.16	108.37±4.39
Ca	72.61±1.03	72.30±1.12	68.87±2.70	64.53±3.69	60.30±2.18	51.15±0.74	54.38±1.11	13.18±0.42
P	31.08±0.62	30.69±0.35	29.59±0.21	26.82±0.18	23.30±0.16	20.37±0.14	16.23±0.12	11.44±0.11

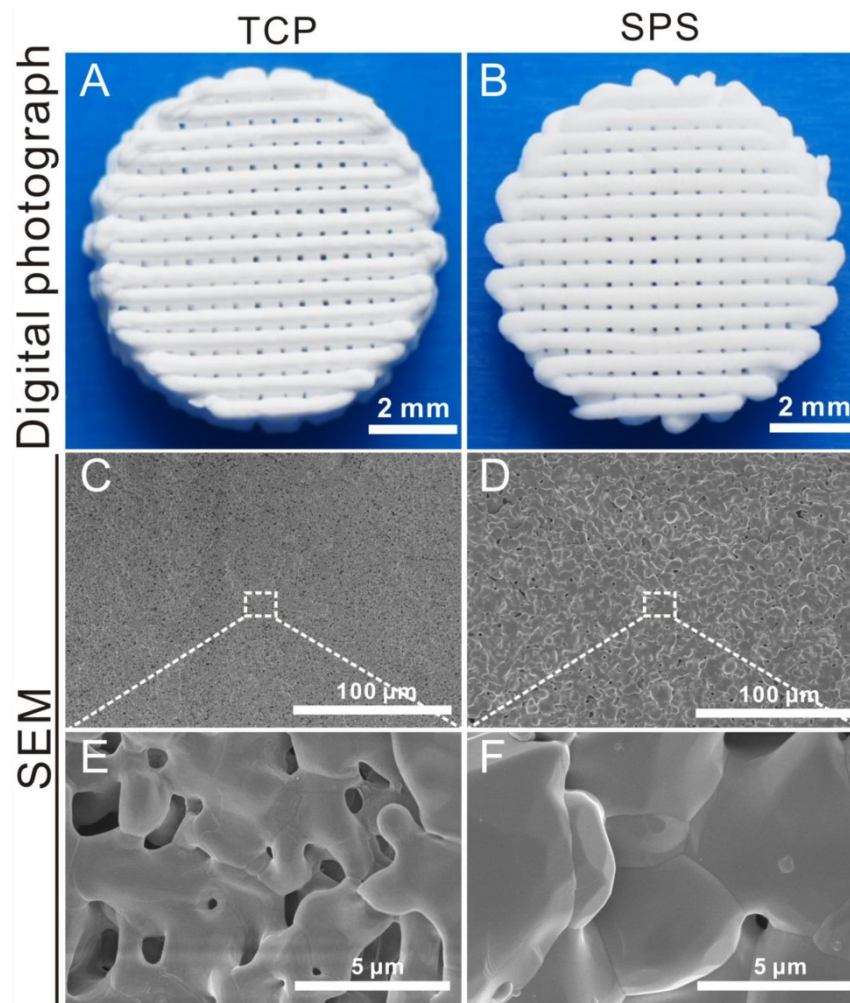


Figure 1. The overview and SEM images of TCP and SPS scaffolds. (A, B) Gross morphology, (C-F) SEM images. The prepared 3D-plotted TCP and SPS scaffolds with controlled pore size (~100 μm) and strut size (~300 μm). The size of crystalline grains in SPS scaffolds was above 5 μm, which was much greater than that of TCP scaffolds.

The underlying mechanism of Sr and Si ions preserving chondrocytes from osteoarthritis

To further elucidate the mechanism of Sr and Si ions preserving chondrocytes from OA, the expression of hedgehog signaling pathway and autophagy related genes, as well as chondrocyte metabolic activity related genes was evaluated (Figure 7 and Figure 8). IL-1 β plays a key role in OA pathogenesis, SANT-1 is a hedgehog signaling inhibitor. Sr and Si ions significantly down-regulated the expression of hedgehog pathway (IHH, Patched-1,

Gli-1) and suppressed chondrocyte metabolic activity related genes (MMP3, MMP13, Adamts-5) within the concentration range of Sr ions 0.25-4 mg/L or Si ions 0.5-8 mg/L. Moreover, Sr and Si ions cooperatively inhibited the hedgehog pathway related genes (IHH, Patched-1, Gli-1) and MMP13 gene expression within the concentration range of Sr ions 0.25-4 mg/L and Si ions 0.5-8 mg/L to protect chondrocytes from OA. In addition, the inhibitory effect on hedgehog pathway was superior to that of SNAT-1 at the concentration of Sr ions 1 mg/L and Si ions 4 mg/L.

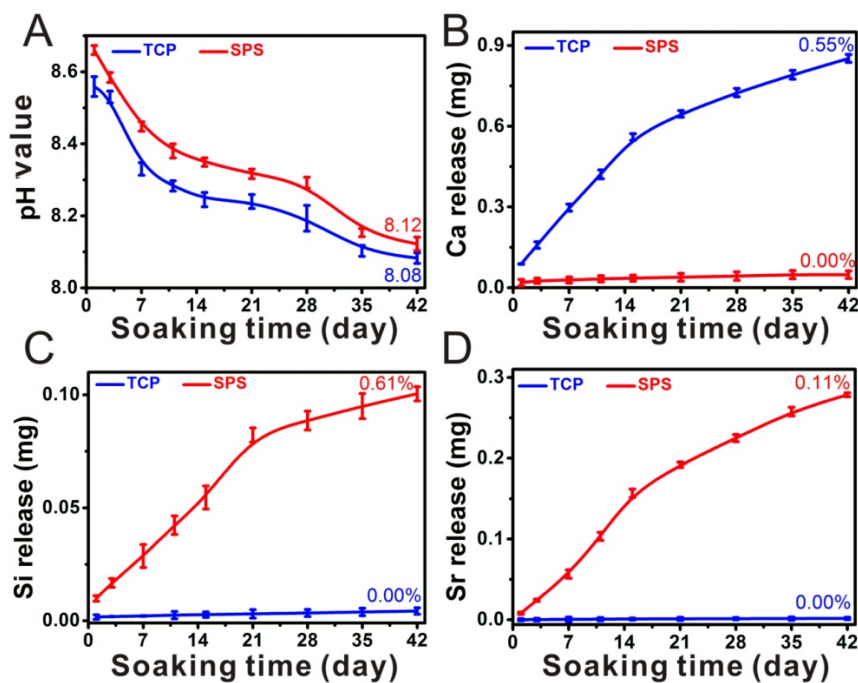


Figure 2. Characterization of SPS scaffolds. The pH value (A), the accumulative release profiles of Ca (B), Si (C) and Sr (D) in DMEM. DMEM is a kind of basic cell culture medium. The pH value of DMEM after soaking TCP and SPS scaffolds was close to the original pH value of DMEM. The original pH value of DMEM is ~8.2. The accumulative released quantity of Ca, Si and Sr from SPS scaffolds showed a steady rise. The accumulative release rate of Ca in TCP and SPS scaffolds was 0.55% and 0.00%, respectively. The accumulative release rate of Si and Sr in SPS scaffolds was 0.61% and 0.11% respectively, while there was no Si and Sr released from TCP scaffolds. Repeat number: n=3.

Additionally, Sr or Si ions significantly enhanced the expression of autophagy related markers (P62, Atg5, Atg12 and Atg16L1) within the concentration range of Sr 0.25-4 mg/L or Si 0.5-8 mg/L (Figure 8). Furthermore, Sr and Si ions together promoted the expression of P62 gene at the concentration of Sr 4 mg/L and Si 8 mg/L, as well as enhanced Atg5 gene expression at the concentration of Sr 1 mg/L and Si 2 mg/L. In addition, Sr and Si ions cooperatively promoted the expression of Atg12 gene within the concentration range of Sr 0.25-4 mg/L and Si 0.5-8 mg/L.

Chondrocytes response in SPS scaffolds *in vitro*

As compared to TCP scaffolds, the proliferation of chondrocytes in SPS scaffolds was significantly enhanced (Figure 9E). Morphology and attachment of chondrocytes in SPS scaffolds were detected with SEM and CLSM (Figure 9). SEM images exhibited that chondrocytes had close contact with SPS scaffolds by numerous filopodia, while the chondrocytes in TCP scaffolds had less filopodia. CLSM images displayed that there were more chondrocytes evenly spread in SPS scaffolds as compared to the TCP scaffolds where chondrocytes were observed.

SPS scaffolds stimulated the *in vivo* osteochondral defects regeneration

To further study the *in vivo* stimulatory efficacy of SPS scaffolds for osteochondral defects, a rabbit

osteochondral defect model was used. Figure 10 showed the overall observation and Micro-CT analysis of specimens collected at 8 and 12 weeks. There was no inflammatory reaction in all specimens, and well-integrated tissue was found in SPS group, while discontinuous tissue was found in the rest of specimens (Figure 10A₁-F₁). The defects in SPS group were filled with well-integrated newly formed bone and cartilage-like tissues at both 8 and 12 weeks, while the defects of TCP and CTR groups remained empty and discontinuous. The Micro-CT analysis displayed that much more calcified tissue was found in TCP and SPS groups as compared to CTR group (Figure 10A₂-F₄). In addition, the trabecula thickness (Tb.Th) and relative bone volume fraction (BV/TV) in the specimens of SPS group were significantly elevated as compared to CTR and TCP groups at week 8 and 12 (Figure S3).

To further evaluate the stimulatory effect of SPS scaffolds for osteochondral defect reconstruction, histological analysis included H&E (Hematoxylin-eosin), S-O (Safranin O/Fast Green) (Figure 11) and TB (Toluidine Blue) (Figure S4) staining, was conducted. H&E staining showed that considerable fibrous tissue formation and poor bone reconstruction as well as large residual void space was found in the CTR group at week 8 and 12 (Figure 11G_{1,2} and J_{1,2}). A mixture of neo-bone and fibrous tissues as well as residual void space was found in TCP group (Figure

1H_{1,2} and K_{1,2}), while a large amount of newly formed bone tissue was found in the defect region of SPS group at 12weeks (Figure 11I_{1,2} and L_{1,2}). Safranin-O/Fast Green staining showed SPS group possessed a certain amount of hyaline cartilage-like tissue, which was more than that of the CTR group, and the new hyaline cartilage-like tissue of the SPS

group has no significant distinction with that of pure TCP group at 8 weeks (Figure 11A₁-C₃). The CTR and TCP groups exhibited a mixture of fibrous tissue and hyaline cartilage-like tissue in the discontinuous defect region at 12weeks, while the SPS group was filled with considerable amount of hyaline cartilage-like tissue (Figure 11D₁-F₃).

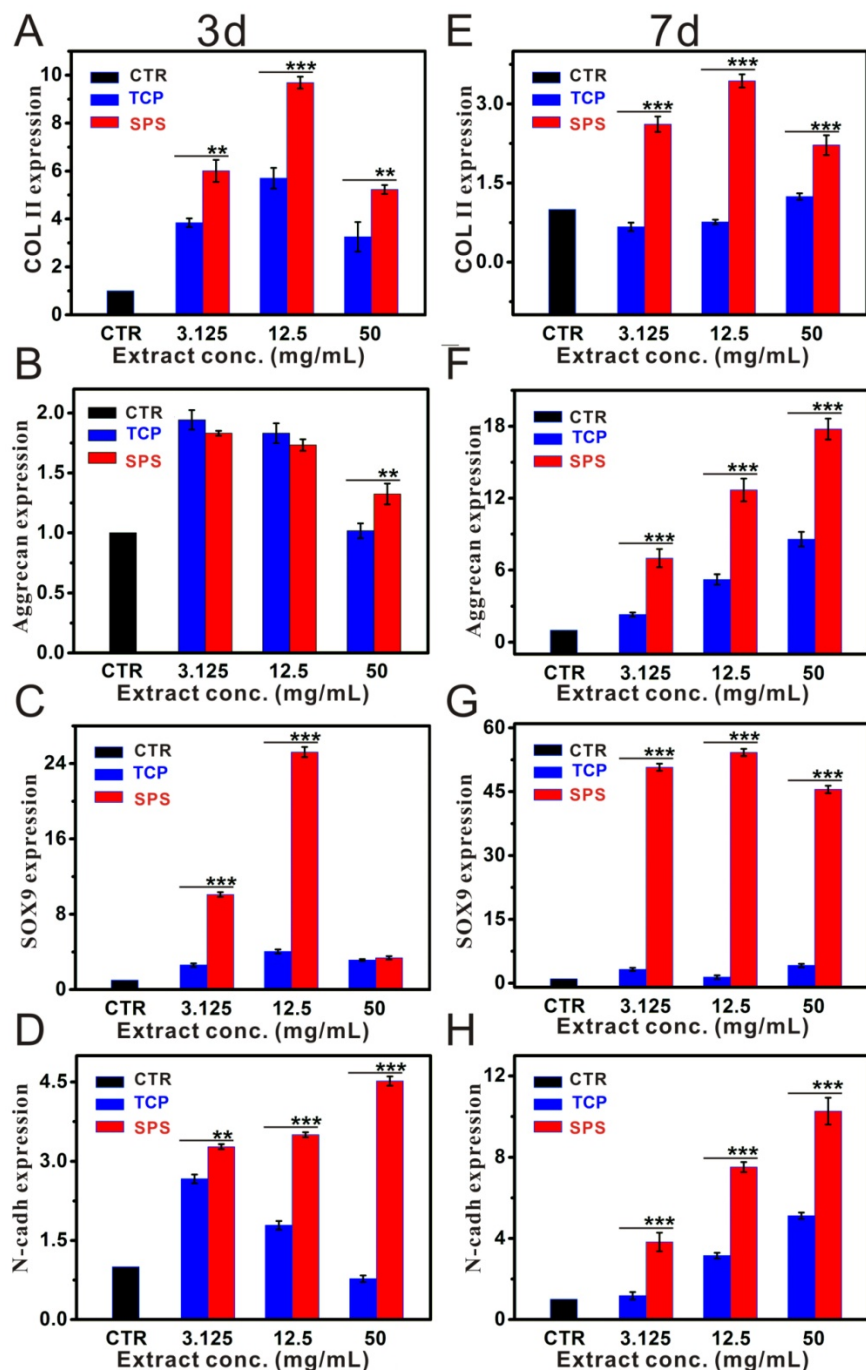


Figure 3. The relative genes expression level of chondrocytes cultured with SPS extracts. The expression of COL II gene (A, E), Aggrecan gene (B, F), SOX9 gene (C, G) and N-cadh gene (D, H) in chondrocytes post culturing with SPS extracts for 3 and 7 days, respectively. SPS extracts distinctly elevated the chondrocytes specified genes (COL II, SOX9 and N-cadh) expression within the concentration range of 3.125-50 mg/mL at day 3 and 7, as compared to that of CTR and TCP groups. Also, Aggrecan gene expression was significantly enhanced as compared to TCP extracts after co-culturing for 7 days within the whole experimental concentration range. The relative gene amount of CTR groups was set as 1, the value of expression gene was the fold change relative to CTR. Repeat number: n=3. (*p<0.05, **p<0.01, ***p<0.001).

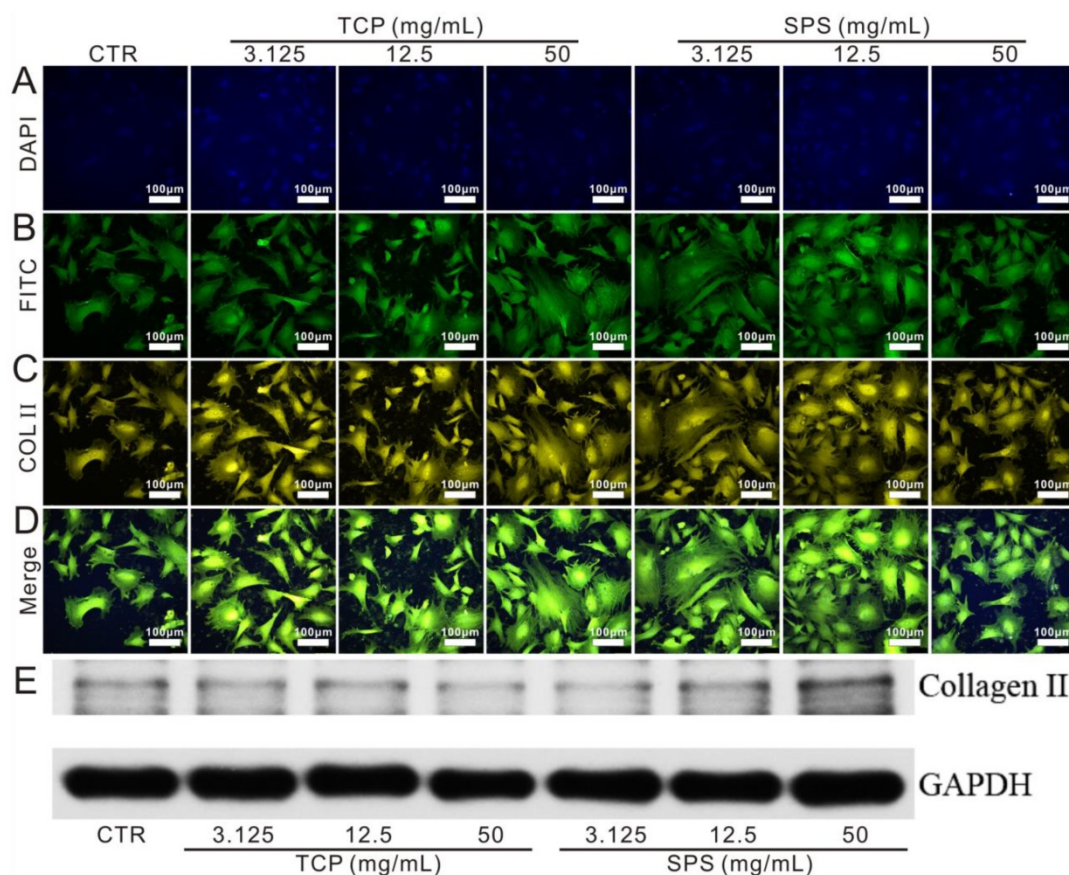


Figure 4. The expression of COL II protein in chondrocytes cultured with TCP and SPS extracts. (A) DAPI, (B) FITC, (C) COL II, (D) merge images, (E) western blot. The expression of COL II protein was enhanced significantly in SPS group (50 mg/mL) as compared to TCP and CTR groups. CTR stands for blank control.

Moreover, calcified tissue and tide mark were found in SPS group at 12 weeks, which demonstrated natural continuous structure between hyaline cartilage and neo-subchondral bone which was highly similar to the natural tissue (Figure 11F₁₋₃), while CTR and TCP groups exhibited disorder and discontinuous structure between cartilage and neo-bone. The Toluidine blue stained analysis was shown in Figure S4. At 8 weeks, a mixture of fibrous tissue and neo-bone tissue was found in CTR and TCP groups, while considerable amount of neo-bone tissue was found in the SPS group. At 12 weeks, partial repair of the defect with hyaline cartilage and subchondral bone was observed at the periphery of the defect in the CTR group, while the surfaces of defect region in TCP and SPS groups were covered with well-integrated hyaline cartilage tissue. Nevertheless, the subchondral bone tissue in TCP group was disordered and uneven, while SPS group showed an orderly continuous and smooth structure between cartilage and neo-bone in subchondral bone. In addition, histological scoring assessment was processed to measure the quantity of neo-cartilage

tissue. SPS group exhibited a higher ICRS (International Cartilage Repair Society) score than CTR and TCP groups (Figure S5).

Discussion

In this study, bioactive SPS scaffolds were applied to regenerate osteochondral defect *in vivo*. It was found that SPS scaffolds were a reliable platform for delivering Sr and Si ions. The Sr and Si ions released from SPS bioactive ceramics promoted chondrocyte maturation *in vitro*, and protected the chondrocytes from OA. Interestingly, SPS scaffolds possessed the ability of promoting the reconstruction of cartilage and subchondral bone tissues simultaneously, as well as restoring the complex interfaces between them. The underlying mechanism may be related to Sr and Si stimulating cartilage reconstruction through activating HIF pathway and promoting subchondral bone regeneration by activation of the Wnt pathway, as well as preserving chondrocytes from OA via increasing autophagy and inhibiting hedgehog pathway.

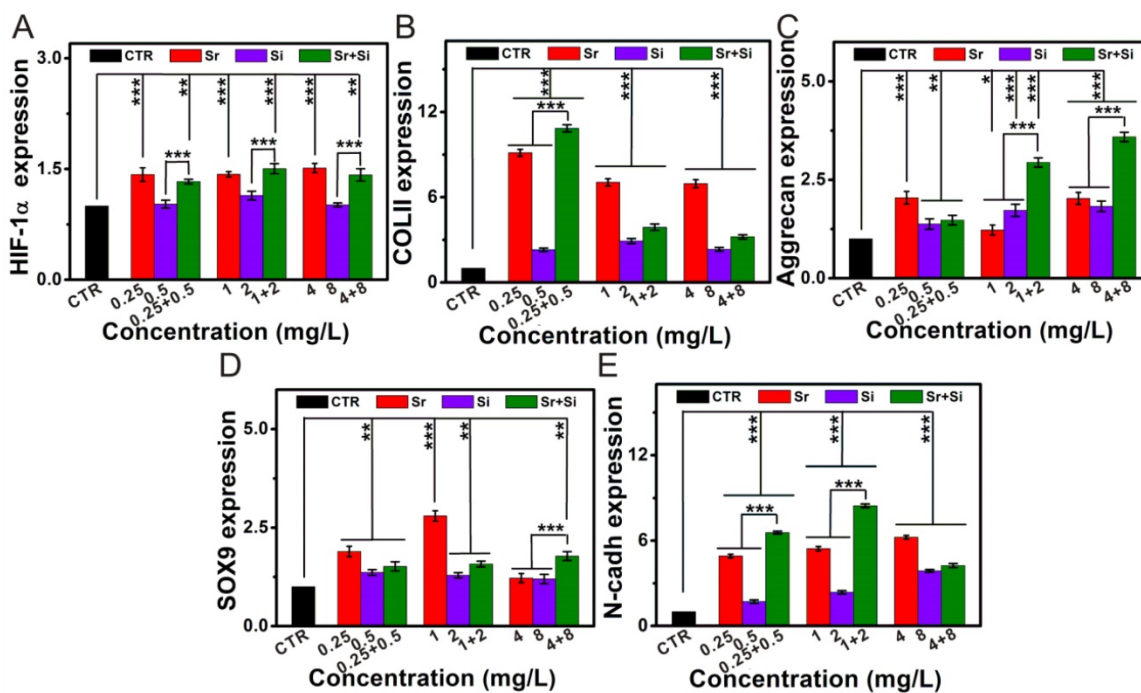


Figure 5. The stimulatory effect of Sr and/or Si ions on chondrocyte maturation. (A) HIF-1α gene, (B) COL II gene, (C) Aggrecan gene, (D) SOX9 gene, (E) N-cadh gene. Sr ions increased chondrocyte specified gene expression through activating HIF-1α pathway within the concentration range of 0.25-4 mg/L. Furthermore, Sr and Si ions markedly enhanced COL II, Aggrecan, SOX9, N-cadh expression within the concentration range of Sr ions 0.25-4 mg/L and Si ions 0.5-8 mg/L, respectively. In addition, the expression of COL II gene was up-regulated by Sr and Si ions together at the concentration of Sr ions 0.25 mg/L and Si ions 0.5 mg/L. The expression level of Aggrecan gene was stimulated by Sr and Si ions cooperatively within the concentration range of Sr ions 1-4 mg/L and Si ions 2-8 mg/L, and the expression of SOX9 gene was elevated by Sr and Si ions at the concentration of Sr ions 4 mg/L and Si ions 8 mg/L. Also, N-cadh gene was enhanced by Sr and Si ions cooperatively within the concentration range of Sr ions 0.25-2 mg/L and Si ions 0.5-4 mg/L. The relative gene amount of CTR groups was set as 1, the value of expression gene was the fold change relative to CTR. Repeat number: n=3. (*p<0.05, **p<0.01, ***p<0.001).

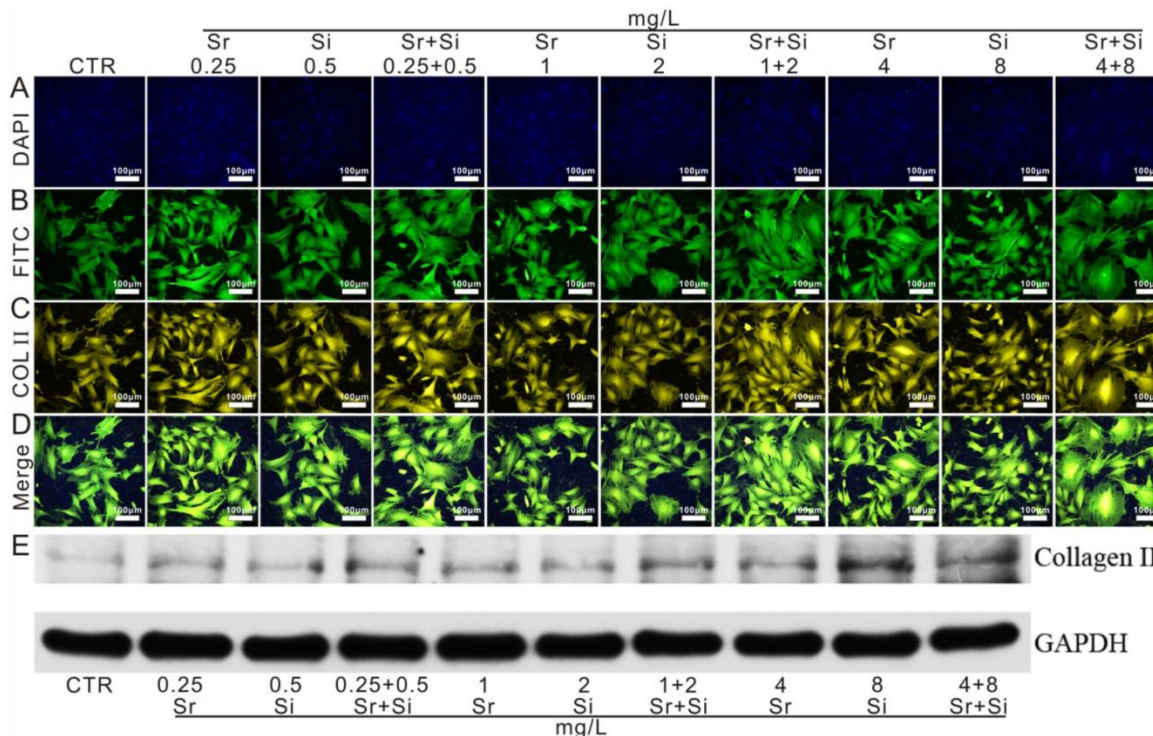


Figure 6. The expression of COL II in chondrocytes cultured with different concentrations of Sr and/or Si ions. (A) DAPI, (B) FITC, (C) COL II, (D) merge images, (E) western blot. COL II protein expression in chondrocytes elevated distinctly cultured with Sr (0.25-4 mg/L) or Si (0.5-8 mg/L) as compared to the CTR group. Furthermore, Sr and Si together promoted COL II protein expression within the concentration range of Sr 0.25-1 mg/L and Si 0.5-2 mg/L. CTR stands for blank control.

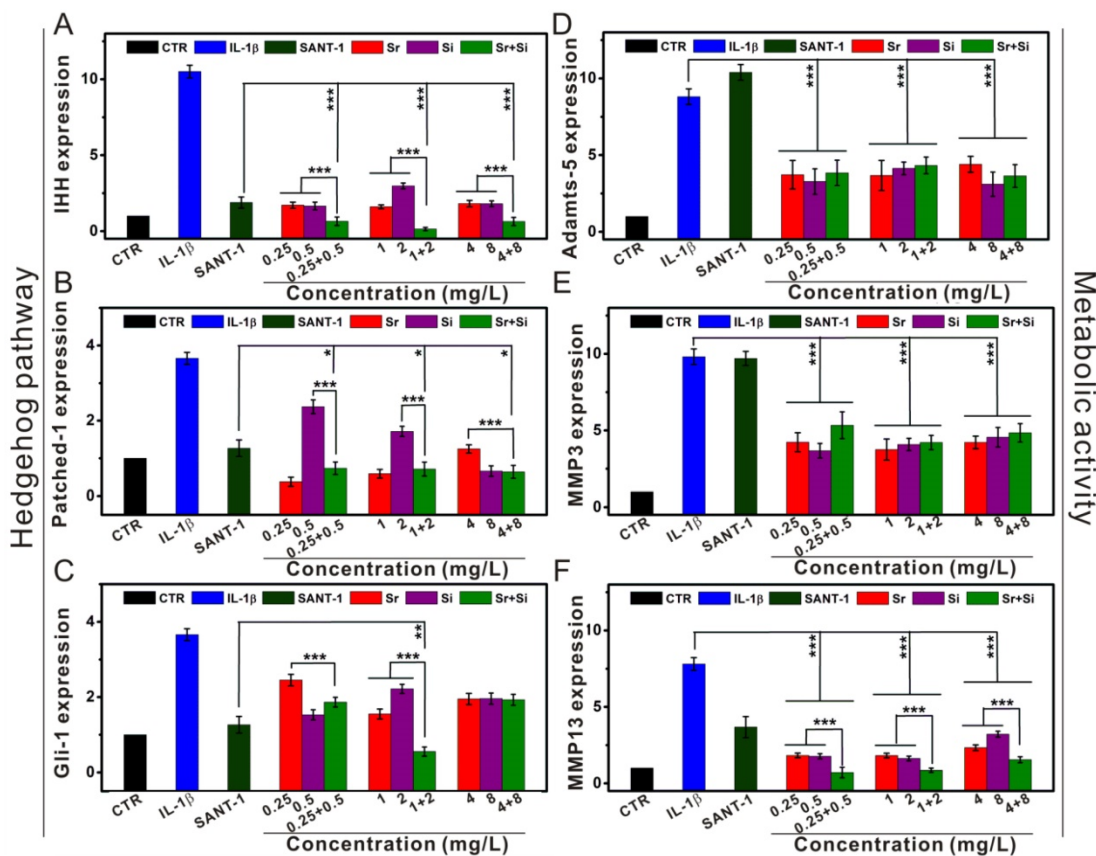


Figure 7. The inhibitory effect of Sr and/or Si ions on hedgehog pathway and metabolic activity in OA chondrocytes. (A) IHH gene, (B) Patched-1 gene, (C) Gli-1 gene, (D) Adams-5 gene, (E) MMP3 gene, (F) MMP13 gene. In OA model, Sr or Si ions protected chondrocytes by inhibiting the hedgehog pathway and metabolic activity within the concentration range of Sr 0.25-4 mg/L or Si 0.5-8 mg/L. Furthermore, Sr and Si ions together inhibited the hedgehog pathway, as well as down-regulated MMP13 gene expression within the concentration range of Sr 0.25-4 mg/L and Si 0.5-8 mg/L to protect chondrocytes from OA. In addition, the inhibitory effect on hedgehog pathway was superior to that of SNAT-1 at the concentration of Sr 1 mg/L and Si 4 mg/L. IL-1 β plays a key role in OA pathogenesis, SANT-1 is a hedgehog signaling inhibitor. The relative gene amount of CTR groups was set as 1, the value of expression gene was the fold change relative to CTR. Repeat number: n=3. (*p<0.05, **p<0.01, ***p<0.001).

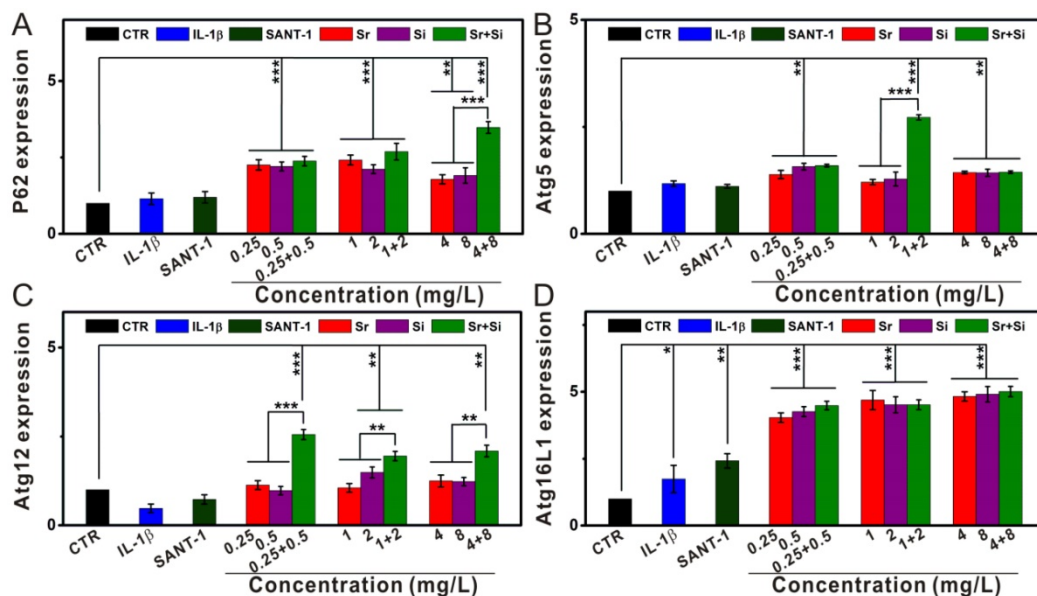


Figure 8. The activation effect of Sr and/or Si ions on autophagy in OA chondrocytes. (A) P62 gene, (B) Atg5 gene, (C) Atg12 gene, (D) Atg16L1 gene. In OA model, Sr or Si ions protected chondrocytes by inducing autophagy within the concentration range of Sr 0.25-4 mg/L or Si 0.5-8 mg/L. Furthermore, Sr and Si ions together promoted the expression of P62 gene at the concentration of Sr 4 mg/L and Si 8 mg/L, as well as enhanced Atg5 gene expression at the concentration of Sr 1 mg/L and Si 2 mg/L. In addition, Sr and Si ions cooperatively promoted the expression of Atg12 gene within the concentration range of Sr 0.25-4 mg/L and Si 0.5-8 mg/L. Sr and/or Si ions protected chondrocytes from OA by increasing autophagy. IL-1 β plays a key role in OA pathogenesis, SANT-1 is a hedgehog signaling inhibitor. The relative gene amount of CTR groups was set as 1, the value of expression gene was the fold change relative to CTR. Repeat number: n=3. (*p<0.05, **p<0.01, ***p<0.001).

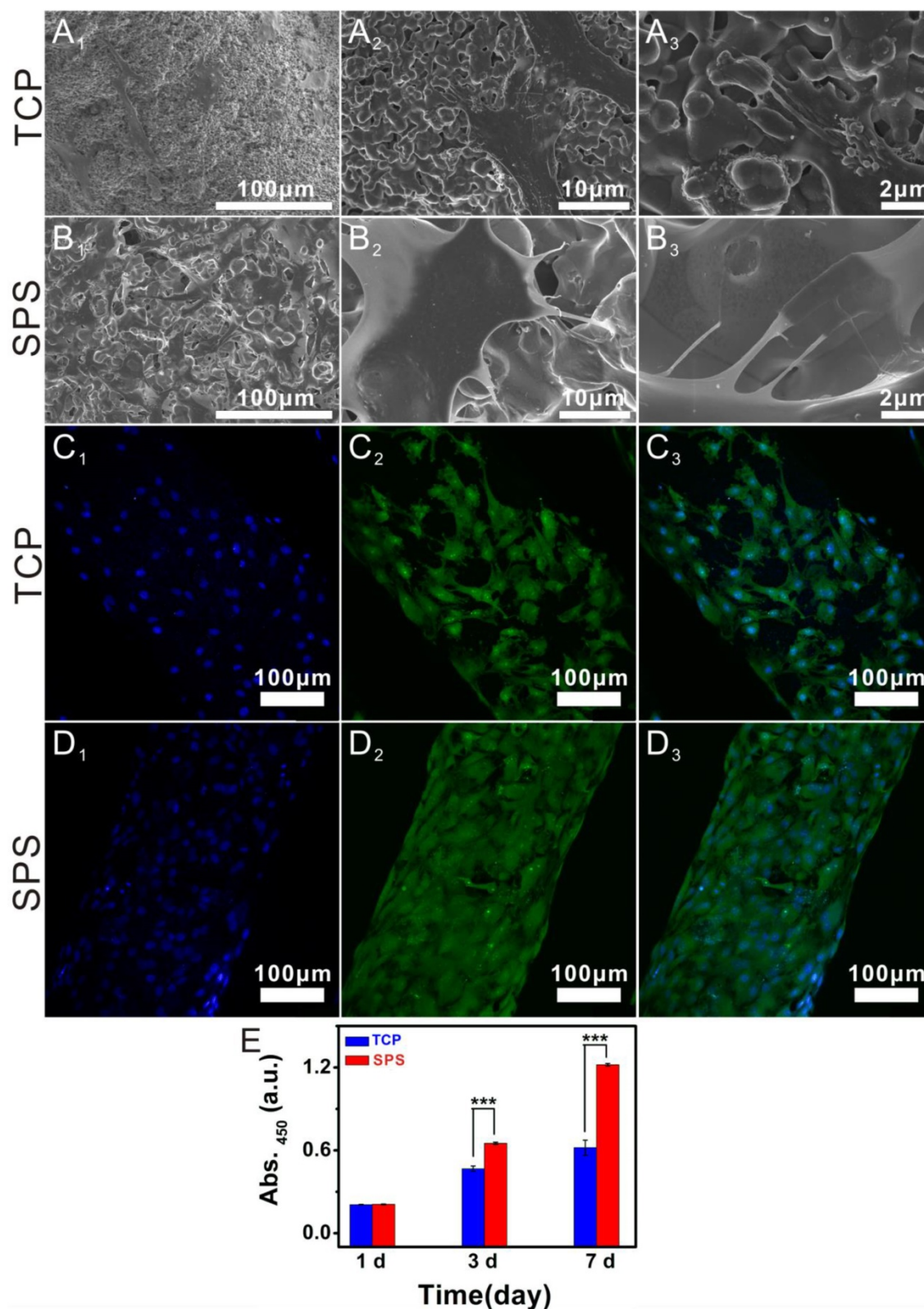


Figure 9. The attachment and morphology of chondrocytes cultured in SPS scaffolds. SEM images showed that chondrocytes attached to TCP scaffolds (A₁-A₃) and SPS scaffolds (B₁-B₃). CLSM images exhibited the morphology and cytoskeleton of chondrocytes cultured in TCP scaffolds (C₁-C₃) and SPS scaffolds (D₁-D₃). A₁ and B₁: 500×, A₂ and B₂: 3,000×, A₃ and B₃: 10,000×; C₁ and D₁: DAPI, C₂ and D₂: FITC, C₃ and D₃: merge images. (E) The proliferation of chondrocytes cultured in SPS and TCP scaffolds. Both TCP and SPS scaffolds supported the attachment of chondrocytes, and the chondrocytes in SPS scaffold exhibited better-defined microfilaments and cytoskeletons as compared to that of TCP scaffold. Compared with TCP scaffolds, SPS scaffolds distinctly elevated chondrocyte proliferation at 3 and 7 days. Repeat number: n=6. (*p<0.05, **p<0.01, ***p<0.001).

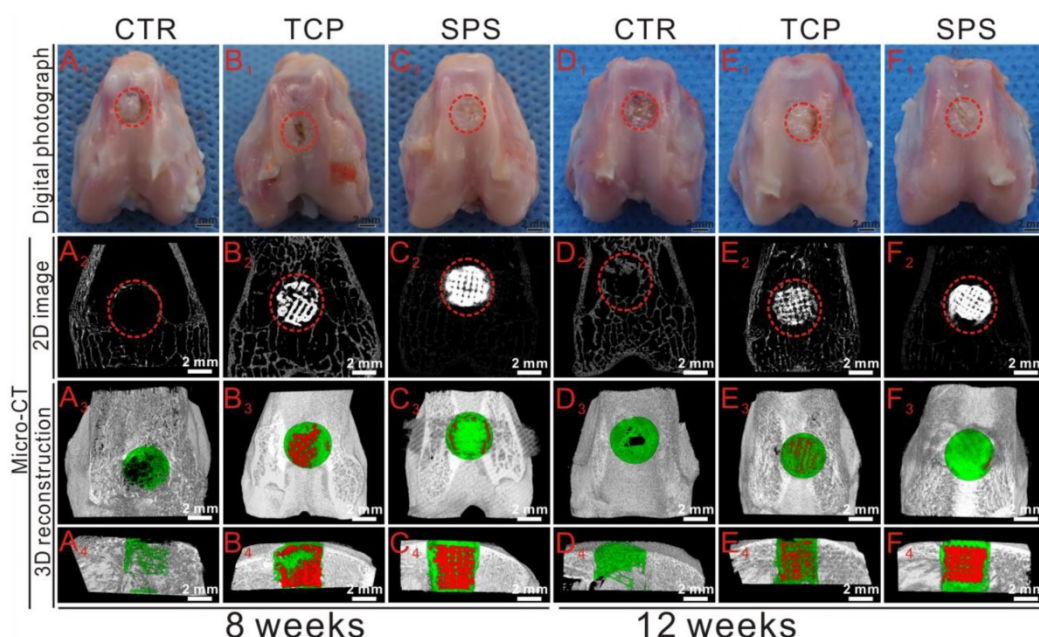


Figure 10. The overall photographs and Micro-CT imaging analysis of the defects at 8 and 12 weeks post-surgery. (A₁-F₁) The gross morphology of the defects, (A₂-F₂) 2D projection images of the defects. (A₃-F₃) and (A₄-F₄) showed the transverse view and sagittal view of 3D construction images. In 2D projection images, the off-white color and white color stand for primary bone and scaffolds, respectively. In 3D reconstruction images, the off-white color, green color and red color stand for primary bone, new bone and scaffold, respectively. As compared to CTR and TCP groups, Micro-CT analysis of defect space exhibited distinctly greater level of bone formation in the SPS group.

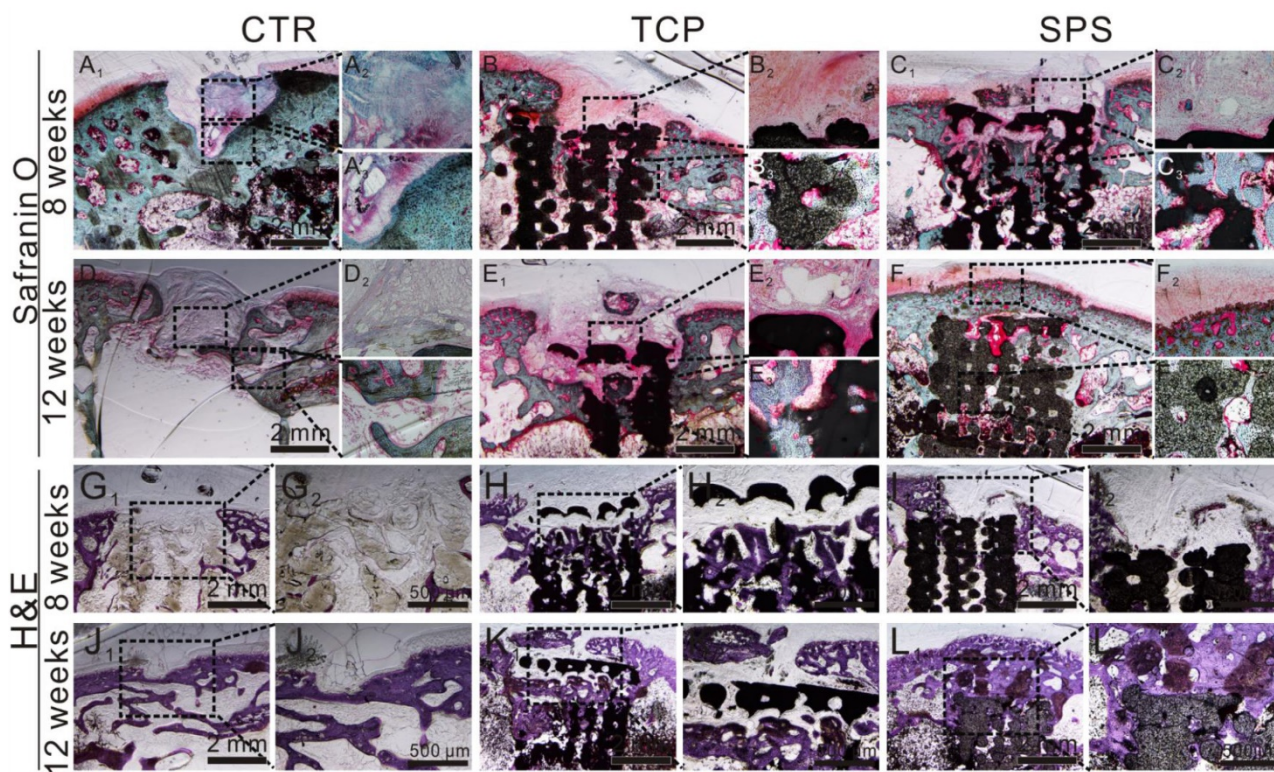


Figure 11. The cartilage and subchondral bone regeneration *in vivo*. (A₁-F₃) Safranin-O/Fast Green staining at 8 (A₁-C₃) and 12 weeks (D₁-F₃) of post-surgery. A_{1,2,3} and D_{1,2,3}: CTR group, B_{1,2,3} and E_{1,2,3}: TCP group, C_{1,2,3} and F_{1,2,3}: SPS group. (G₁-L₂) H&E staining at 8 weeks (G₁-L₂) and 12 weeks (J₁-L₂) of post-surgery. G_{1,2} and J_{1,2}: CTR group, H_{1,2} and K_{1,2}: TCP group, I_{1,2} and L_{1,2}: SPS group. Safranin-O/Fast Green staining showed SPS groups possessed a certain amount of hyaline cartilage-like tissue, which was more than that of the CTR group and has no significant distinction with that of pure TCP group at 8 weeks. However, CTR and TCP groups exhibited a mixture of fibrous tissue and hyaline cartilage-like tissue in the discontinuous defect region at 12 weeks, while that of SPS group was filled with considerable amount of hyaline cartilage-like tissue. Moreover, SPS group displayed well-integrated and orderly continuous structure between cartilage and neo-bone, while CTR and TCP groups exhibited disordered and discontinuous structure between cartilage and neo-bone. H&E staining indicated that the defect region of SPS group was filled with a great amount of bony tissue at 12 weeks, and that of pure TCP group possessed less and incomplete bony tissue, while CTR group displayed a mixture of fibrous and bony tissue in the defect region.

In our study, SPS extracts significantly enhanced SOX9 production, following by elevating Aggrecan, COL II, N-cadh genes expression, as well as

increasing COL II protein expression in chondrocytes. Furthermore, TCP extracts promoted the chondrogenic genes expression, which was consistent

with the previous studies [32, 33]. Previously, calcium (Ca) ions could promote the proliferation and differentiation of tissue cells, as well as have a positive effect on chondrocytes and cartilage [34, 35]. Consequently, the calcium ions in TCP extracts may have a positive effect on enhancing the expression of chondrogenic genes. Previously, the foundation for chondrocytes regeneration and matrix synthesis for cartilage reconstruction could be prepared via activating HIF signal pathway to improve the SOX9 and other related genes (Aggrecan, COL II and N-cadh) expression [36-40]. Furthermore, autophagy is of great importance for maintaining cartilage balance [41]. Additionally, hedgehog pathway plays an important role in OA onset and development via regulating the expression of the IHH gene [42-46]. Consequently, it is probable that Sr and Si ions released from SPS bio-ceramics stimulated chondrocytes maturation and promoted cartilage regeneration via activating HIF signal pathway, and protected chondrocytes from OA by suppressing chondrocyte metabolic activity and increasing autophagy as well as inhibiting hedgehog pathway.

To test this hypothesis, the related genes of HIF pathway (HIF-1 α), hedgehog signal pathway (IHH, Patched-1 and Gli-1) and metabolic activity (MMP3, MMP13 and Adamts-5), as well as autophagy related markers (P62, Atg5, Atg12 and Atg16L1) were investigated. The results indicated that Sr stimulated HIF-1 α , COL II, SOX9, Aggrecan and N-cadh genes expression within the concentration range of 0.25-4 mg/L. Interestingly, the expression of COL II, SOX9, Aggrecan and N-cadh genes was stimulated by Sr and Si ions together within the whole experimental concentration range (Sr 0.25-4 mg/L and Si 0.5-8 mg/L), and the expression of COL II protein was also elevated within the same concentration range. In OA development, the related genes of metabolic activity (MMP3, MMP13 and Adamts-5) and hedgehog signal pathway (IHH, Patched-1 and Gli-1) were over-expression. Within the whole experimental concentration range, hedgehog pathway and metabolic activity induced by IL-1 β were inhibited, while autophagy was increased. In an *in vitro* OA model, Sr and Si ions inhibited IHH, Patched-1, Gli-1 and MMP13 expression. Furthermore, the expression of P62 gene (Sr 4 mg/L and Si 8 mg/L) and Atg5 gene (Sr 1 mg/L and Si 2 mg/L) was cooperatively promoted at a specific concentration. In addition, Sr and Si ions together promoted the expression of Atg12 gene within the whole experimental concentration range. More interestingly, the inhibitory effect of Sr combined with Si ions on hedgehog pathway was superior to SANT-1. It was reported that SANT-1 could protect

cartilage from degradation via inhibiting hedgehog pathway [47-49]. On the basis of these studies, it is reasonable to conclude that the Sr and Si ions released from SPS scaffolds promoted chondrocytes maturation *in vitro* and stimulated cartilage lesion regeneration *in vivo* via activation of HIF pathway, and protected chondrocytes from OA by suppressing chondrocytes metabolic activity and increasing autophagy as well as inhibiting hedgehog pathway.

Interestingly, SPS scaffolds not only promoted the regeneration of cartilage, but also stimulated the reconstruction of subchondral bone *in vivo*. In this study, the histological analysis and Micro-CT results indicated that SPS scaffolds significantly promoted the subchondral bone regeneration as compared to TCP scaffolds, gold standard bio-ceramic scaffolds for bone regeneration. Series of studies demonstrated that Sr could promote bone formation *in vitro* and *in vivo* [50-52]. Furthermore, it was reported that Sr and Si-containing bioactive ceramics could enhance bone regeneration [51]. Additionally, Sr has been proved to stimulate the osteogenic differentiation of MSCs by up-regulating extracellular matrix (ECM) gene expression and activating Wnt/ β -catenin pathway [53]. It was also reported that Si stimulated MSCs differentiation by activating Wnt pathways [54, 55]. Hence, it is reasonable to speculate that in this study, Sr and Si ions released from SPS bioactive scaffold may together contribute to promote subchondral bone regeneration via activation of the Wnt pathway.

In clinic, medicines such as strontium ranelate or smoothed antagonist are used for OA therapy. Whereas these medicines may lead to osteophyte overgrowth and reduce subchondral bone remodeling, as well as other serious side-effects. Furthermore, various kinds of scaffolds have been fabricated for reconstruction of osteochondral defects, for example biphasic scaffolds, triphasic scaffolds and other multilayered scaffolds. However, these constructions could not biologically mimic the original structure and functional characteristics of osteochondral tissue. Although many BMSCs-specific-affinity peptides and signaling molecules have been incorporated into scaffolds to promote osteochondral defect reconstruction, these strategies often induce various side effects. For instance, some peptides can specifically recognize and recruit pluripotent stem cells as well as promote osteogenesis in subchondral bone, which has the potential to increase cartilage calcification [15, 56, 57]. Some molecules which could preserve cartilage from degradation, such as TGF- β signaling trigger molecules, may trigger osteoarthritis via perturbing subchondral bone homeostasis [58-60]. There are few reports that used one single scaffold for regeneration of both cartilage and subchondral bone

simultaneously, as well as restored the complex interface microstructure between them. The osteochondral interface is described by the interaction of calcified cartilage and the underlying subchondral bone. Structurally, osteochondral interface includes tidemark and calcified cartilage. Hereupon, a single type and bi-lineage SPS scaffold containing multi-bioactive ions was applied to regenerate osteochondral defect *in vivo*. Compared with traditional therapy, such as oral administration medicines, SPS scaffolds acted in a local scope and avoided systemic toxicity, and Sr combined with Si ions inhibited on hedgehog pathway was superior to SNAT-1 (hedgehog signaling inhibitor). Furthermore, SPS scaffolds with monophasic structure could avert the delamination issues, which are superior to multilayered scaffolds. Additionally, SPS scaffolds well regenerated the tidemark and calcified cartilage in the osteochondral interface. On the basis of the *in vitro* and *in vivo* physiological studies, it is probable that Sr and Si ions stimulating cartilage reconstruction may activate HIF pathway and promote subchondral bone regeneration by activation of Wnt pathway, and further protect chondrocytes from OA via suppressing chondrocytes metabolic activity and increasing autophagy as well as inhibiting hedgehog pathway together.

Conclusion

Hereupon, SPS scaffolds were successfully fabricated by a modified 3D-printing method, which enabled sustained release of Sr and Si ions *in situ*. The released Sr and Si ions promoted chondrocyte maturation and preserved chondrocytes from OA, as well as stimulated cartilage and subchondral bone regeneration. The underlying mechanisms might refer to Sr and Si ions stimulating cartilage reconstruction by activating HIF pathway and promoting subchondral bone regeneration through activation of Wnt pathway, as well as preserving chondrocytes from OA via activating autophagy and inhibiting hedgehog pathway. Consequently, bioactive SPS scaffolds possess bi-lineage bio-activities for regeneration of osteochondral interface between cartilage and subchondral bone, which is beneficial for OA therapy and regeneration of osteochondral defects by harnessing multi-bioactive ions in a monophasic scaffold.

Abbreviations

BV/TV: bone volume fraction; CAD: computer assist design; CCK-8: cell counting kit-8; CLSM: confocal laser scanning microscope; COL II: type II collagen protein; CTR: control group; DAPI: 4',6-diamidino-2-phenylindole; DMEM: dulbecco's

modified eagle's medium low-glucose; F-127: poloxamer; FITC: fluorescein isothiocyanate phalloidin; HE: hematoxylin-eosin; HMDS: hexamethyldisilazane; ICPAES: inductively coupled plasma atomic emission spectroscopy; ICRS: international cartilage repair society; IHH: indian hedgehog; IL-1 β : interleukin-1 β ; Micro-CT: micro-computed tomography; NH₄H₂PO₄: ammonium dihydrogen phosphate; OA: osteoarthritis; rBMSCs: rabbit mesenchymal stem cells; RT-qPCR: quantitative real-time reverse transcriptase polymerase chain reaction; Safranin-O: safranin-O/Fast green; SANT-1: smoothened antagonist; SD: standard deviation; SEM: scanning electron microscope; Si: silicon; SiO₂: silicon dioxide; SPS: Sr₅(PO₄)₂SiO₄; Sr: strontium; SrO: strontium oxide; TB: toluidine blue; TCP: tricalciumphosphate; Tr. Th: trabecular thickness.

Acknowledgements

This work was supported by the National Key Research and Development Program of China (2016YFB0700803), the Natural Science Foundation of China (51761135103, 81771989, 81601612), Key Research Program of Frontier Sciences CAS (QYZDB-SSW-SYS027), Science and Technology Commission of Shanghai Municipality (17441903700, 16DZ2260603) and Key Research Program of Science & Technology Support Program of Jiangsu Province (BE2016763).

Supplementary Material

Supplementary figures and tables.

<http://www.thno.org/v08p1940s1.pdf>

Competing Interests

The authors have declared that no competing interest exists.

References

- Mow VC, Ratcliffe A, Poole AR. Cartilage and diarthrodial joints as paradigms for hierarchical materials and structures. *Biomaterials*. 1991; 13: 67-97.
- Tao SC, Yuan T, Zhang YL, Yin WJ, Guo SC, Zhang CQ. Exosomes derived from miR-140-5p-overexpressing human synovial mesenchymal stem cells enhance cartilage tissue regeneration and prevent osteoarthritis of the knee in a rat model. *Theranostics*. 2017; 7: 180-195.
- Sellam J, Berenbaum F. The role of synovitis in pathophysiology and clinical symptoms of osteoarthritis. *Nat Rev Rheumatol*. 2010; 6: 625-635.
- Steadman JR, Sterett WI. The surgical treatment of knee injuries in skiers. *Med Sci Sports Exerc*. 1995; 27: 328-333.
- Liu X, Jin X, Ma PX. Nanofibrous hollow microspheres self-assembled from star-shaped polymers as injectable cell carriers for knee repair. *Nat Mater*. 2011; 10: 398-408.
- Das RK, Gocheva V, Hammink R, Zouani OF, Rowan AE. Stress-stiffening-mediated stem-cell commitment switch in soft responsive hydrogels. *Nat Mater*. 2016; 15: 318-325.
- LopaSilvia, MadryHenning. Bioinspired Scaffolds for Osteochondral Regeneration. *Tissue Eng Part A*. 2014; 20: 2052-2076.
- Burr DB, Gallant MA. Bone remodelling in osteoarthritis. *Nat Rev Rheumatol*. 2012; 8: 665-673.
- Fan W, Wu C, Miao X, Liu G, Saifzadeh S, Sugiyama S, et al. Biomaterial scaffolds in cartilage-subchondral bone defects influencing the repair of autologous articular cartilage transplants. *J Biomater Appl*. 2013; 27: 979-989.

10. Wu Y, Zhu S, Wu C, Lu P, Hu C, Xiong S, et al. A Bi - Lineage Conductive Scaffold for Osteochondral Defect Regeneration. *Adv Funct Mater.* 2014; 24: 4473-4483.
11. Castro NJ, Patel R, Zhang LG. Design of a Novel 3D Printed Bioactive Nanocomposite Scaffold for Improved Osteochondral Regeneration. *Cell Mol Bioeng.* 2015; 8: 416-432.
12. Shimomura K, Moriguchi Y, Murawski CD, Yoshikawa H, Nakamura N. Osteochondral tissue engineering with biphasic scaffold: current strategies and techniques. *Tissue Eng Part B Rev.* 2014; 20: 468-476.
13. Liu M, Yu X, Huang F, Cen S, Zhong G, Xiang Z. Tissue engineering stratified scaffolds for articular cartilage and subchondral bone defects repair. *Orthopedics.* 2013; 36: 868-873.
14. Yu P, Ning C, Zhang Y, Tan G, Lin Z, Liu S, et al. Bone-Inspired Spatially Specific Piezoelectricity Induces Bone Regeneration. *Theranostics.* 2017; 7: 3387-3397.
15. Hu X, Wang Y, Tan Y, Wang J, Liu H, Yang S, et al. A Difunctional Regeneration Scaffold for Knee Repair based on Aptamer-Directed Cell Recruitment. *Adv Mater.* 2017; 29: 1605235.
16. Kandel RA, Grynblas M, Pilliar R, Lee J, Wang J, Waldman S, et al. Repair of osteochondral defects with biphasic cartilage-calcium polyphosphate constructs in a Sheep model. *Biomaterials.* 2006; 27: 4120-4131.
17. Chen J, Chen H, Li P, Diao H, Zhu S, Dong L, et al. Simultaneous regeneration of articular cartilage and subchondral bone in vivo using MSCs induced by a spatially controlled gene delivery system in bilayered integrated scaffolds. *Biomaterials.* 2011; 32: 4793-4805.
18. Terra J, Dourado ER, Eon JG, Ellis DE, Gonzalez G, Rossi AM. The structure of strontium-doped hydroxyapatite: an experimental and theoretical study. *Phys Chem Chem Phys.* 2009; 11: 568-577.
19. Bonnelye E, Chabadel A, Saltel F, Jurdic P. Dual effect of strontium ranelate: stimulation of osteoblast differentiation and inhibition of osteoclast formation and resorption in vitro. *Bone.* 2008; 42: 129-138.
20. Marie PJ, Hott M, Modrowski D, De PC, Guillemain J, Deloffre P, et al. An uncoupling agent containing strontium prevents bone loss by depressing bone resorption and maintaining bone formation in estrogen-deficient rats. *J Bone Miner Res.* 1993; 8: 607-615.
21. Marie PJ, Felsenberg D, Brandi ML. How strontium ranelate, via opposite effects on bone resorption and formation, prevents osteoporosis. *Osteoporos Int.* 2011; 22: 1659-1667.
22. Yu DG, Ding HF, Mao YQ, Liu M, Yu B, Zhao X, et al. Strontium ranelate reduces cartilage degeneration and subchondral bone remodeling in rat osteoarthritis model. *Acta Pharmacol Sin.* 2013; 34: 393-402.
23. Okita N, Honda Y, Kishimoto N, Liao W, Azumi E, Hashimoto Y, et al. Supplementation of strontium to a chondrogenic medium promotes chondrogenic differentiation of human dedifferentiated fat cells. *Tissue Eng Part A.* 2015; 21: 1695-1704.
24. Pietak AM, Reid JW, Stott MJ, Sayer M. Silicon substitution in the calcium phosphate bioceramics. *Biomaterials.* 2007; 28: 4023-4032.
25. Carlisle EM. Silicon: a possible factor in bone calcification. *Science.* 1970; 167: 279-280.
26. Calomme MR, Vanden Berghe DA. Supplementation of calves with stabilized orthosilicic acid. Effect on the Si, Ca, Mg, and P concentrations in serum and the collagen concentration in skin and cartilage. *Biol Trace Elem Res.* 1997; 56: 153-165.
27. Hott M, De PC, Modrowski D, Marie PJ. Short-term effects of organic silicon on trabecular bone in mature ovariectomized rats. *Calcif Tissue Int.* 1993; 53: 174-179.
28. Nielsen FH, Poellot R. Dietary silicon affects bone turnover differently in ovariectomized and sham-operated growing rats. *J Trace Elem Exp Med.* 2004; 17: 137-149.
29. Valerio P, Pereira MM, Goes AM, Leite MF. The effect of ionic products from bioactive glass dissolution on osteoblast proliferation and collagen production. *Biomaterials.* 2004; 25: 2941-2948.
30. Ramaswamy Y, Wu C, Hummel AV, Combes V, Grau G, Zreiqat H. The responses of osteoblasts, osteoclasts and endothelial cells to zirconium modified calcium-silicate-based ceramic. *Biomaterials.* 2008; 29: 4392-4402.
31. Horecka A, Hordyjewska A, Blicharski T, Kocot J, Żelazowska R, Lewandowska A, et al. Simvastatin Effect on Calcium and Silicon Plasma Levels in Postmenopausal Women with Osteoarthritis. *Biol Trace Elem Res.* 2016; 171: 1-5.
32. Wang SQ, Xia J, Chen J, Lu JX, Wei YB, Chen FY, et al. Influence of biological scaffold regulation on the proliferation of chondrocytes and the repair of articular cartilage. *Am J Transl Res.* 2016; 8: 4564-4573.
33. Guo XM, Wang CY, Zhang YF, Xia RY, Hu M, Duan CM, et al. Repair of large articular cartilage defects with implants of autologous mesenchymal stem cells seeded into beta-tricalcium phosphate in a sheep model. *Tissue Eng.* 2004; 10: 1818-1829.
34. Wang L, Shelton RM, Cooper PR, Lawson M, Triffitt JT, Barralet JE. Evaluation of sodium alginate for bone marrow cell tissue engineering. *Biomaterials.* 2003; 24: 3475-3481.
35. Nishida T, Kubota S, Aoyama E, Yamanaka N, Lyons KM, Takigawa M. Low-intensity pulsed ultrasound (LIPUS) treatment of cultured chondrocytes stimulates production of CCN family protein 2 (CCN2), a protein involved in the regeneration of articular cartilage: mechanism underlying this stimulation. *Osteoarthritis Cartilage.* 2017; 25: 759-769.
36. Bouaziz W, Sigaux J, Modrowski D, Devignes CS, Funck-Brentano T, Richette P, et al. Interaction of HIF1 α and β -catenin inhibits matrix metalloproteinase 13 expression and prevents cartilage damage in mice. *Proc Natl Acad Sci U S A.* 2016; 113: 5453-5458.
37. Pfander D, Cramer T, Schipani E, Johnson RS. HIF-1 α controls extracellular matrix synthesis by epiphyseal chondrocytes. *J Cell Sci.* 2003; 116: 1819-1826.
38. Ferguson C, Alpern E, Miclau T, Helms JA. Does adult fracture repair recapitulate embryonic skeletal formation? *Mech Dev.* 1999; 87: 57-66.
39. Komatsu DE, Hadjiargyrou M. Activation of the transcription factor HIF-1 and its target genes, VEGF, HO-1, iNOS, during fracture repair. *Bone.* 2004; 34: 680-688.
40. Wan C, Gilbert SR, Wang Y, Cao X, Shen X, Ramaswamy G, et al. Activation of the Hypoxia-Inducible Factor-1 α Pathway Accelerates Bone Regeneration. *Proc Natl Acad Sci U S A.* 2008; 105: 686-691.
41. Caramés B, Taniguchi N, Otsuki S, Blanco FJ, Lotz M. Autophagy is a protective mechanism in normal cartilage, and its aging-related loss is linked with cell death and osteoarthritis. *Osteoarthritis Cartilage.* 2010; 62: 791-801.
42. Tchetaina EV, Squires G, Poole AR. Increased type II collagen degradation and very early focal cartilage degeneration is associated with upregulation of chondrocyte differentiation related genes in early human articular cartilage lesions. *J Rheumatol.* 2005; 32: 876-886.
43. Zhou J, Chen Q, Lanske B, Fleming BC, Terek R, Wei X, et al. Disrupting the Indian hedgehog signaling pathway in vivo attenuates surgically induced osteoarthritis progression in Col2a1-CreERT2; Ihh(floxed/floxed) mice. *Arthritis Res Ther.* 2014; 16: R11.
44. Lin AC, Seeto BL, Bartoszko JM, Khoury MA, Whetstone H, Ho L, et al. Modulating hedgehog signaling can attenuate the severity of osteoarthritis. *Nat Med.* 2009; 15: 1421-1425.
45. Wei F, Zhou J, Wei X, Zhang J, Fleming BC, Terek R, et al. Activation of Indian hedgehog promotes chondrocyte hypertrophy and upregulation of MMP-13 in human osteoarthritic cartilage. *Osteoarthritis Cartilage.* 2012; 20: 755-763.
46. Zhang C, Wei X, Chen C, Cao K, Li Y, Jiao Q, et al. Indian hedgehog in synovial fluid is a novel marker for early cartilage lesions in human knee joint. *Int J Mol Sci.* 2014; 15: 7250-7265.
47. Thompson CL, Wiles A, Poole CA, Knight MM. Lithium chloride modulates chondrocyte primary cilia and inhibits Hedgehog signaling. *FASEB J.* 2015; 30: 716-726.
48. Fleury A, Hoch L, Martinez MC, Faure H, Taddei M, Petricci E, et al. Hedgehog associated to microparticles inhibits adipocyte differentiation via a non-canonical pathway. *Sci Rep.* 2016; 6: 23479.
49. Ruiz-Heiland G, Horn A, Zerr P, Hofstetter W, Baum W, Stock M, et al. Blockade of the hedgehog pathway inhibits osteophyte formation in arthritis. *Ann Rheum Dis.* 2012; 71: 400-407.
50. Zhang W, Shen Y, Pan H, Lin K, Liu X, Darvell BW, et al. Effects of strontium in modified biomaterials. *Acta Biomater.* 2011; 7: 800-808.
51. Zhu Y, Zhu M, He X, Zhang J, Tao C. Substitutions of strontium in mesoporous calcium silicate and their physicochemical and biological properties. *Acta Biomater.* 2013; 9: 6723-6731.
52. Lin K, Xia L, Li H, Jiang X, Pan H, Xu Y, et al. Enhanced osteoporotic bone regeneration by strontium-substituted calcium silicate bioactive ceramics. *Biomaterials.* 2013; 34: 10028-10042.
53. Yang F, Yang D, Tu J, Zheng Q, Cai L, Wang L. Strontium enhances osteogenic differentiation of mesenchymal stem cells and in vivo bone formation by activating Wnt/ β -catenin signaling. *Stem Cells.* 2011; 29: 981-991.
54. Liu D, Yi C, Fong CC, Jin Q, Wang Z, Yu WK, et al. Activation of multiple signaling pathways during the differentiation of mesenchymal stem cells cultured in a silicon nanowire microenvironment. *Nanomedicine.* 2014; 10: 1153-1163.
55. Sun T, Wang M, Shao Y, Wang L, Zhu Y. The Effect and Osteoblast Signaling Response of Trace Silicon Doping Hydroxyapatite. *Biol Trace Elem Res.* 2017; 181: 1-13.
56. Shi W, Sun M, Hu X, Ren B, Cheng J, Li C, et al. Structurally and Functionally Optimized Silk-Fibroin-Gelatin Scaffold Using 3D Printing to Repair Cartilage Injury In Vitro and In Vivo. *Adv Mater.* 2017; 29: 1701089.
57. Chen Y, Liu X, Liu R, Gong Y, Wang M, Huang Q, et al. Zero-order controlled release of BMP2-derived peptide P24 from the chitosan scaffold by chemical grafting modification technique for promotion of osteogenesis in vitro and enhancement of bone repair in vivo. *Theranostics.* 2017; 7: 1072-1087.
58. Wang M, Sampson ER, Jin H, Jia L, Qiao HK, Im HJ, et al. MMP13 is a critical target gene during the progression of osteoarthritis. *Arthritis Res Ther.* 2013; 15: R5.
59. Zhen G, Wen C, Jia X, Li Y, Crane JL, Mears SC, et al. Inhibition of TGF- β signaling in mesenchymal stem cells of subchondral bone attenuates osteoarthritis. *Nat Med.* 2013; 19: 704-712.
60. Chen Z, Xing L, Fan Q, Cheetham AG, Lin R, Holt B, et al. Drug-Bearing Supramolecular Filament Hydrogels as Anti-Inflammatory Agents. *Theranostics.* 2017; 7: 2003-2014.